

Numerical models of protoneutron stars and type-II supernovae — recent developments

H.-Thomas Janka

Max-Planck-Institut für Astrophysik
Karl-Schwarzschild-Str. 1, D-85740 Garching, Germany
email: thj@mpa-garching.mpg.de

ABSTRACT

The results of recent multi-dimensional simulations of type-II supernovae are reviewed. They show that convective instabilities in the collapsed stellar core might play an important role already during the first second after the formation of the supernova shock. Convectively unstable situations occur below and near the neutrinosphere as well as in the neutrino-heated region between the nascent neutron star and the supernova shock after the latter has stalled at a radius of typically 100–200 km.

While convective overturn in the layer of neutrino energy deposition clearly helps the explosion to develop and potentially provides an explanation of strong mantle and envelope mixing, asphericities, and non-uniform ^{56}Ni distribution observed in supernova SN 1987A, its presence and importance depends on the strength of the neutrino heating and thus on the size of the neutrino fluxes from the neutron star. Convection in the hot-bubble region can only develop if the growth timescale of the instabilities and the heating timescale are both shorter than the accretion timescale of the matter advected through the stagnant shock. For too small neutrino luminosities this requirement is not fulfilled and convective activity cannot develop, leading to very weak explosions or even fizzling models, just as in the one-dimensional situation.

Convectively enhanced neutrino luminosities from the protoneutron star can therefore provide an essential condition for the explosion of the star. Very recent two-dimensional, self-consistent, general relativistic simulations of the cooling of a newly-formed neutron star demonstrate and confirm the possibility that Ledoux convection, driven by negative lepton number and entropy gradients, may encompass the whole protoneutron star within less than one second and can lead to an increase of the neutrino fluxes by up to a factor of two.

1. Introduction

Neutrinos play a crucial role in our understanding of type-II supernova explosions. According to the currently most widely accepted theory for the explosion of a massive star, the explosion energy is provided by the neutrinos that are abundantly emitted

from the nascent neutron star and interact at a probability between 1% and 10% with the material of the progenitor star. This energy deposition is not only supposed to power the propagation of the supernova shock into the stellar mantle and envelope regions and to cause the violent disruption of the star, but also drives a mass outflow from the surface of the protoneutron star that continues for more than 10 seconds and which might be a suitable site for r-process nucleosynthesis (Woosley & Hoffman 1992, Witt et al. 1994, Takahashi et al. 1994, Woosley et al. 1994). The emission of electron lepton number and energy via neutrinos determines the evolution of the hot, collapsed stellar core towards the cold deleptonized neutron star remnant. Moreover, the interactions of neutrinos with target nuclei and nucleons in the neutrino-driven wind and in the stellar mantle can have important implications for supernova nucleosynthesis. Last but not least, the ~ 20 neutrinos detected in the Baksan (Alexeyev 1988), Kamiokande (Hirata et al. 1987), and IMB laboratories (Bionta et al. 1987) in connection with SN 1987A were the first experimental confirmation of our theoretical picture of the events that precede the explosion of a massive star. Still they serve as a tool to constrain theories of neutrino properties and particle physics at the extreme conditions of nascent neutron stars.

As discussed in detail in Lecture 1, the neutrino emission from the newly born neutron star is characterized by the following properties. Electron neutrinos are emitted from the neutrinosphere with a typical energy of about 10 MeV, while electron antineutrinos have about 50% higher energies and muon and tau neutrinos are radiated with even higher mean energies. This can be easily be understood by the fact that ν_e and $\bar{\nu}_e$ experience charged-current interactions while ν_μ and ν_τ do not. In addition, due to the neutron-proton asymmetry of the medium the coupling of $\bar{\nu}_e$ to the medium via absorptions onto protons is less strong than ν_e absorptions onto the more abundant neutrons. Despite the different temperatures of their emission spectra, all kinds of neutrinos have roughly similar (say, within a factor of 2) luminosities during most of the Kelvin-Helmholtz cooling phase of the protoneutron star. Because the transport of ν_μ and ν_τ is strongly affected by isoenergetic scatterings off n and p , their characteristic spectral temperatures and effective temperatures are significantly different. The neutrino spectra are not thermal (“blackbody”) spectra, but are pinched with a depletion in both the low-energy part and the high-energy tail. This depletion can be accounted for by using Fermi-Dirac distributions to describe the emission spectra at a certain time, and introducing an effective spectral degeneracy parameter of order unity (typically about 3–5 for ν_e , 2–3 for $\bar{\nu}_e$, and between 0 and 2 for $\nu_x \equiv \nu_\mu, \bar{\nu}_\mu, \nu_\tau, \bar{\nu}_\tau$).

About 99% of the total gravitational binding energy that is set free during the collapse of the stellar iron core and the formation of the neutron star is emitted in neutrinos, only about 1% ends up in the kinetic energy of the supernova explosion, and even less, only about 0.01% accounts for the spectacularly bright outburst of light that is seen as type-II supernova event on the sky. Despite the enormous amount of energy that is available from the gravitational collapse, it is not easy to channel the mentioned $\sim 1\%$ or about 10^{51} erg into kinetic energy. It is still an unresolved question how type-II manage to do this. It is generally accepted nowadays that for “reasonable” nuclear equations of state and core masses of the progenitor star the prompt or hydrodynamical mechanism does not work: The supernova shock formed at the moment of core bounce is too weak to overcome the huge energy losses due

to the disintegration of Fe group nuclei and additional neutrino losses. The shock stagnates before it reaches the surface of the stellar Fe core. During the following several hundred milliseconds of evolution, neutrinos deposit energy behind the shock. If this neutrino heating is strong enough, the shock can gain so much energy that it is “revived” and can indeed disrupt the star (see Lecture 1 and the references given there).

However, the neutrino-matter coupling is so weak that this “delayed” or neutrino-driven mechanism seems to be extremely sensitive to small changes of the physics inside the collapsed stellar core. In particular, if the neutrino fluxes do not surpass a certain threshold value, the explosion becomes too weak to be compatible with observations or even fizzles. Where are the uncertainties of our current knowledge of the physics inside stellar iron cores and what might be the missing link to a stable and robust explosion mechanism? What could help the neutrino-driven mechanism? Do current models underestimate the neutrino flux from the neutron star or do they treat the neutrino-matter coupling in the heating region incorrectly?

2. Different possibilities

There are different lines of exploration currently followed up by the supernova group at the MPI für Astrophysik in Garching and by other groups in Livermore, Los Alamos, and Oak Ridge. On the one hand, these activities focus on a closer investigation of the neutrino interactions and neutrino transport in the protoneutron star. On the other hand, they concentrate on the simulations of the hydrodynamical evolution of the collapsed star in more than one spatial dimension.

2.1 Lower neutrino opacities in the protoneutron star?

So far, the theoretical understanding of neutrino interactions with target nuclei and nucleons in a dense environment is incomplete and detailed calculations of the neutrino opacity of a nuclear medium including particle correlation and screening effects are not yet available. For that reason, partly also motivated and justified by the effort to simplify the numerical description, all current supernova codes employ neutrino reaction rates calculated for interactions with isolated target particles. At least, the rates are more or less reliably corrected for blocking effects in the fermion phase spaces. The real situation may be largely different and more complicated.

For example, Raffelt & Seckel (1991) considered auto-correlation effects for the nucleon spins which can lead to a dramatic reduction of the axial-vector neutral current (and possibly also charged current) cross sections. Rapid nucleon spin fluctuations of the scattering nucleons lead to a reduced effective spin “seen” by the neutrino as a reaction partner. In a parametric study, Keil et al. (1995) and Janka et al. (1996) have investigated the effects on the neutrino cooling of newly formed neutron stars and found a nearly linear decrease of the cooling time of the protoneutron star with the global reduction factor for the opacities. This is a non-trivial result because with reduced opacities also the deleptonisation of the star is accelerated. As a result of this, the star heats up faster and to higher peak temperatures. Since the opacities increase with the temperature (neutrino energy), the net effect on the cooling of the star is not obvious. Keil et al. (1995) also found that the emitted

neutrinos become more energetic when the opacity of the protoneutron star is lower and the neutrinosphere moves deeper into the star.

The combined effects, reduced cooling time and increased mean spectral neutrino energies, lead to a distortion of the predicted neutrino signal which can be compared with the neutrino burst observed in the Kamiokande II and IMB detectors in connection with SN 1987A. Keil et al. (1995) concluded that a reduction of the opacities by more than a factor of 2 seems quite unlikely unless the late and low-energy neutrino events in Kamiokande 2 and IMB are discarded as background or unless they can be explained by some non-standard neutrino emission process, e.g., associated with accretion or a spontaneous, first-order phase transition in the supranuclear matter that might occur after several seconds of Kelvin-Helmholtz cooling of the newly born neutron star. Despite a lot of vague speculations, there is no qualified and theoretically founded model for such events in or at the protoneutron star that can explain the involved energies, timescales, and structure of the neutrino signal. For a summary and discussion of some of the addressed aspects, see Janka (1995).

The derived lower bound for the reduction of the neutrino opacity which is still compatible with the SN 1987A neutrino signals sets interesting limits for the nucleon spin fluctuation rate in the supernova core (Janka et al. 1996). The theoretical background and formal justification for such a limit was discussed by Sigl (1996). Although an opacity reduction by a factor of about 2 is by far not as much as allowed from principle physical reasons, a corresponding doubling of the neutrino luminosities from the nascent neutron star would have a very large effect on the supernova explosion. In order to come to definite conclusions, however, more reliable calculations of the neutrino opacities in the dense medium of supernova cores are urgently called for.

2.2 Convection in the protoneutron star?

Alternatively, or in addition, convective processes in the hot and lepton-rich protoneutron star might raise the neutrino fluxes and could thus lead to more favorable conditions for neutrino heating outside the neutrinosphere and could help shock revival.

Epstein (1979) pointed out that not only entropy, S , inversions but also zones in the post-collapse core where the lepton fraction, Y_l , decreases with increasing radius tend to be unstable against Ledoux convection. Negative S and/or Y_l gradients in the neutrinospheric region and in the layers between the nascent neutron star and the weakening prompt shock front were realized in a variety of post-bounce supernova models by Burrows & Lattimer (1988), and after shock stagnation in computations by Hillebrandt (1987) and more recently by Bruenn (1993), Bruenn & Mezzacappa (1994), and Bruenn et al. (1995). Despite different equations of states (EOS), ν opacities, and ν transport methods, the development of negative Y_l and S gradients is common in these simulations and can also be found in protoneutron star cooling models of Burrows & Lattimer (1986), Keil & Janka (1995), and Sumiyoshi et al. (1995).

Convection above the neutrinosphere but below the neutrino-heated region can hardly be a direct help for the explosion (Bethe et al. 1987, Bruenn et al. 1995), whereas convectively enhanced lepton number and energy transport inside the neutrinosphere raise the ν luminosities and can definitely support neutrino-energized

supernova explosions (Bethe et al. 1987). In this context, Burrows (1987) and Burrows & Lattimer (1988) have discussed entropy-driven convection in the protoneutron star on the basis of 1D, general relativistic (GR) simulations of the first second of the evolution of a hot, $1.4 M_{\odot}$ protoneutron star. Their calculations were done with a Henyey-like code using a mixing-length scheme for convective energy and lepton transport. Recent 2D models (Herant et al. 1994, Burrows et al. 1995, Janka & Müller 1996 and references therein) confirmed the possibility that convective processes can occur in the surface region of the protoneutron star immediately after shock stagnation (“prompt convection”) for a period of at least several 10 ms. These models, however, have been evolved only over rather short times or with insufficient numerical resolution in the protoneutron star or with a spherically symmetrical description of the core of the protoneutron star that was in some cases even replaced by an inner boundary condition.

Mayle & Wilson (1988) and Wilson & Mayle (1988, 1993) demonstrated that convection in the nascent neutron star can be a crucial ingredient that leads to successful delayed explosions. With the high-density EOS and treatment of the ν transport used by the Livermore group, however, negative gradients of Y_l tend to be stabilized by positive S gradients (see, e.g., Wilson & Mayle 1989). Therefore they claim doubly diffusive neutron finger convection to be more important than Ledoux convection. Doubts about the presence of doubly diffusive instabilities, on the other hand, were recently raised by Bruenn & Dineva (1996). Bruenn & Mezzacappa (1994) and Bruenn et al. (1995) also come to a negative conclusion about the relevance of prompt convection in the neutrinospheric region. Although their post-bounce models show unstable S and Y_l stratifications, the mixing-length approach in their 1D simulations predicts convective activity inside and around the neutrinosphere to be present only for 10–30 ms after bounce and to have no significant impact on the ν fluxes and spectra when an elaborate multi-group flux-limited diffusion method is used for the ν transfer. Such conclusions seem to be supported by preliminary 2D simulations with the same input physics (Guidry 1996). These 2D models, however, still suffer from the use of an inner boundary condition at a fixed radius of 20–30 km.

From these differing and partly contradictory results it is evident that the question whether, where, when, and how long convection occurs below the neutrinosphere seems to be a matter of the EOS, of the core structure of the progenitor star, of the shock properties and propagation, and of the ν opacities and the ν transport description. In the work which will be reported in Sect. 3.1, we compare 1D simulations with the first self-consistent 2D models that follow the evolution of the newly formed neutron star for more than a second, taking into account the GR gravitational potential and making use of a flux-limited equilibrium diffusion scheme that describes the transport of ν_e , $\bar{\nu}_e$, and ν_x (sum of ν_{μ} , $\bar{\nu}_{\mu}$, ν_{τ} , and $\bar{\nu}_{\tau}$) and is very good at high optical depths but only approximative near the protoneutron star surface (Keil & Janka 1995). Our simulations demonstrate that Ledoux convection may continue in the protoneutron star for a long time and can involve the whole star after about one second.

2.3 Convective instabilities in the neutrino-heated region?

Observations of the light curve and spectra of SN 1987A strongly suggest that convective instabilities and aspherical processes might play an important role not only

inside the nascent neutron star, but also outside of it in its very close vicinity. This is the region where the radioactive elements, in particular ^{56}Ni , which power the supernova light curve, are synthesized during the explosion.

The occurrence of large-scale mixing and overturn processes which must reach deep into the exploding star was clearly indicated by SN 1987A. From the observations we learned that radioactive material had been mixed out with very high velocities from the layers of its formation near the nascent neutron star far into the hydrogen envelope of the progenitor star. This was supported by the early detection of X-rays (Dotani et al. 1987, Sunyaev et al. 1987, Wilson et al. 1988) and γ -emission (Matz et al. 1988, Mahoney et al. 1988, Cook et al. 1988, Sandie et al. 1988, Gehrels et al. 1988, Teegarden et al. 1989) and by the observation of strongly Doppler-shifted and -broadened infrared emission lines of iron group elements (Erickson et al. 1988, Rank et al. 1988, Barthelmy et al. 1989, Witteborn et al. 1989, Haas et al. 1990, Spyromilio et al. 1990, Tueller et al. 1990, Colgan et al. 1994) at a time when the photosphere of the supernova was still well inside the hydrogen envelope. Also, the expanding supernova ejecta developed a clumpy and inhomogeneous structure quite early during the explosion (Li et al. 1993).

Besides direct evidence from SN 1987A, theoretical modelling of the supernova light curve suggested the need for mixing of hydrogen with a large part of the stellar mantle (Arnett 1988, Woosley 1988, Shigeyama et al. 1988, Shigeyama & Nomoto 1990, Arnett et al. 1989). The smoothness of the light curve of SN 1987A provided indirect information about the existence and strength of the mixing process. Mixing of hydrogen towards the center helps to explain the smooth and broad light curve maximum by the time-spread of the liberation of recombination energy. Mixing of heavy elements into the hydrogen-rich envelope homogenizes the opacity and again smooths the light curve. Neither the required amount of mixing nor the observed high velocities of radioactive decay products could be accounted for merely by Rayleigh-Taylor instabilities at composition interfaces in the mantle and envelope of the progenitor star after shock passage (Arnett et al. 1989; Den et al. 1990; Yamada et al. 1990; Hachisu et al. 1990, 1991; Fryxell et al. 1991; Herant & Benz 1991, 1992). Moreover, fast moving, dense explosion fragments outside of the supernova shock front have recently been discovered in the Vela supernova remnant by ROSAT X-ray observations (Aschenbach et al. 1995), revealing a very clumpy and inhomogeneous structure of the Vela and other supernova remnants.

In addition, the increasing number of identified high-velocity pulsars (Harrison et al. 1993, Taylor et al. 1993, Lyne & Lorimer 1994, Frail & Kulkarni 1991, Stewart et al. 1993, Caraveo 1993) might also be interpreted as an aspect of the new picture that type-II supernova explosions are by no means spherically symmetrical events, but that violent processes with noticeable deviation from spherical symmetry take place in the deep interior of the star during the early moments of the explosion.

All this was taken as a serious motivation to extend the modelling of the onset of the explosion to more than one spatial dimension (Herant et al. 1992, 1994; Burrows & Fryxell 1992, 1993; Janka 1993; Janka & Müller 1993, 1994, 1995a, 1996; Müller 1993; Miller et al. 1993; Shimizu et al. 1993, 1994; Yamada et al. 1993; Müller & Janka 1994; Burrows et al. 1995). These numerical models could indeed show that convective overturn in the neutrino-heated region around the protoneutron star can be a crucial help for the explosion. However, it turned out (Janka & Müller 1995a,

Guidry 1996) that even with the helpful effects of convective energy transport from the heating region towards the supernova shock, the neutrino energy deposition and thus the neutrino luminosities from the neutron star have to be larger than some lower threshold. If the heating is not strong enough, hot-bubble convection does not have time to develop on the timescale of the accretion of matter from the shock onto the protoneutron star. In Sect. 3.2 we shall review some of the results of our simulations.

3. Multi-dimensional simulations of convective processes in type-II supernovae

Convection can be driven by a radial gradient of the entropy per nucleon S and/or by a gradient of the lepton number per baryon Y_l (Epstein 1979) where Y_l includes contributions from e^- and e^+ and from ν_e and $\bar{\nu}_e$ if the latter are in equilibrium with the matter. Convective instability in the Ledoux approximation sets in when

$$C_L(r) \equiv \left(\frac{\partial \rho}{\partial S} \right)_{P, Y_l} \frac{dS}{dr} + \left(\frac{\partial \rho}{\partial Y_l} \right)_{P, S} \frac{dY_l}{dr} > 0. \quad (1)$$

There are different regions in the collapsed stellar core where this criterion is fulfilled during different phases of the evolution.

3.1 Two-dimensional simulations of protoneutron star cooling

Simulations of protoneutron star cooling in spherical symmetry were performed by Burrows & Lattimer (1986), Suzuki (1989), and more recently by Keil & Janka (1995) and Sumiyoshi et al. (1995). These models show the development of negative gradients of entropy and lepton fraction as the cooling and deleptonization of the nascent neutron star advances. Keil et al. (1996) therefore attempted to do the first two-dimensional cooling simulations for a period of more than one second after core bounce.

3.1.1 Numerical implementation

The simulations were performed with the explicit Eulerian hydrodynamics code *Prometheus* (Fryxell et al. 1989) that employs a Riemann-solver and is based on the Piecewise Parabolic Method (PPM) of Colella & Woodward (1984). A moving grid with 100 nonequidistant radial zones (initial outer radius ~ 60 km, final radius ~ 20 km) and with up to 60 angular zones was used, corresponding to a radial resolution of a few 100 m ($\lesssim 1$ km near the center) and a maximum angular resolution of 1.5° . In the angular direction, periodic boundary conditions were imposed at $\pm 45^\circ$ above and below the equatorial plane. The stellar surface was treated as an open boundary where the velocity was calculated from the velocity in the outermost grid zone, the density profile was extrapolated according to a time-variable power law, and the corresponding pressure was determined from the condition of hydrostatic equilibrium. The *Prometheus* code was extended for the use of different time steps and angular resolutions in different regions of the star. Due to the extremely restrictive Courant-Friedrichs-Lowy (CFL) condition for the hydrodynamics, the implicit ν

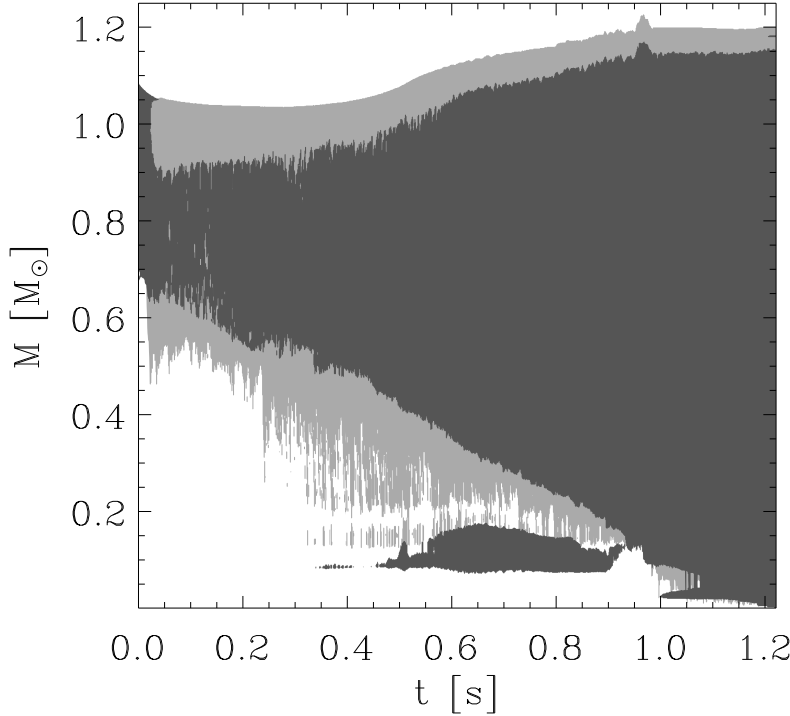


Fig. 1. Convective (baryon) mass region inside the protoneutron star versus time for the 2D simulation. Black indicates regions which are Ledoux unstable or only marginally stable, grey denotes over- and undershooting regions where the absolute value of the angular velocity is $|v_\theta| > 10^7$ cm/s.

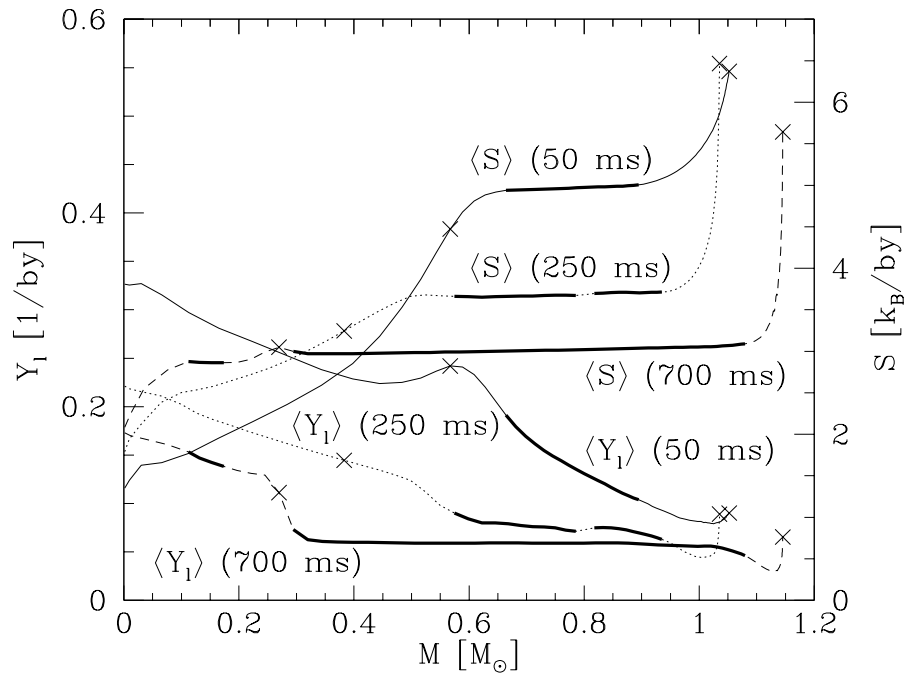


Fig. 2. Angle-averaged S and Y_l profiles in the protoneutron star. Thick solid lines indicate regions that are unstable or only marginally stable against Ledoux convection, crosses mark boundaries of over- and undershooting regions where the absolute value of the angular velocity is $|v_\theta| > 10^7$ cm/s.

transport was computed with typically 10 times larger time steps than the smallest hydrodynamics time step on the grid ($\sim 10^{-7}$ s) (Keil 1996).

Our simulations were started with the $\sim 1.1 M_{\odot}$ (baryonic mass) central, dense part ($\rho \gtrsim 10^{11}$ g/cm³) of the collapsed core of a $15 M_{\odot}$ progenitor star (Woosley et al. 1988) that was computed to a time of about 25 ms after core bounce (i.e., a few ms after the stagnation of the prompt shock) by Bruenn (1993). Accretion was not considered but additional matter could be advected onto the grid through the open outer boundary. In the 2D run, Newtonian asphericity corrections were added to the spherically symmetrical GR gravitational potential: $\Phi_{2D} \equiv \Phi_{1D}^{GR} + (\Phi_{2D}^N - \Phi_{1D}^N)$. This should be a sufficiently good approximation because convective motions produce only local and minor deviations of the mass distribution from spherical symmetry. Using the GR potential ensured that transients due to the mapping of Bruenn's (1993) relativistic 1D results to our code were very small. When starting our 2D simulation, the radial velocity (under conservation of the local specific total energy) was randomly perturbed in the whole protoneutron star with an amplitude of 0.1%. The thermodynamics of the neutron star medium was described by the EOS of Latimer & Swesty (1991) which yields a physically reasonable description of nuclear matter below about twice nuclear density and is thus suitable to describe the interior of the considered low-mass neutron star ($M_{ns} \lesssim 1.2 M_{\odot}$).

The ν transport was carried out in radial direction for every angular zone of the finest angular grid. Angular transport of neutrinos was neglected. This underestimates the ability of moving buoyant fluid elements to exchange lepton number and energy with their surroundings and is only correct if radial radiative and convective transport are faster. Moreover, ν shear viscosity was disregarded. Analytical estimates (see Keil et al. 1996) show that for typically chosen numerical resolution the neutrino viscosity is smaller than the numerical viscosity of the PPM code (which is very small compared to other hydrodynamics codes), but even the numerical viscosity is not large enough to damp out the growth and development of the convective instabilities in the protoneutron star.

3.1.2 Results

Shortly after core bounce, the criterion of Eq. (1) is fulfilled between $\sim 0.7 M_{\odot}$ and $\sim 1.1 M_{\odot}$ (black area in Fig. 1) and convective activity develops within ~ 10 ms after the start of the 2D simulation. About 30 ms later the outer layers become convectively stable which is in agreement with Bruenn & Mezzacappa (1994). In our 2D simulation, however, the convectively unstable region retreats to mass shells $\lesssim 0.9 M_{\odot}$ and its inner edge moves deeper into the neutrino-opaque interior of the star, following a steeply negative lepton gradient that is advanced towards the stellar center by the convectively enhanced deleptonization of the outer layers (Figs. 1 and 2). Note that the black area in Fig. 1 and the thick solid lines in Fig. 2 mark not only those regions in the star which are convectively unstable but also those *which are only marginally stable* according to the Ledoux criterion of Eq. (1) for angle-averaged S and Y_l , i.e., regions where $\mathcal{C}_L(r) \geq a \cdot \max_r(|\mathcal{C}_L(r)|)$ with $a = 0.05$ holds. For $a \lesssim 0.1$ the accepted region varies only little with a and is always embedded by the grey-shaded area where the absolute value of the angular velocity is $|v_{\theta}| > 10^7$ cm/s. Yet, only sporadically and randomly appearing patches in the convective layer fulfill Eq. (1) rigorously. Figure 2 shows that the black region in Fig. 1 coincides with the

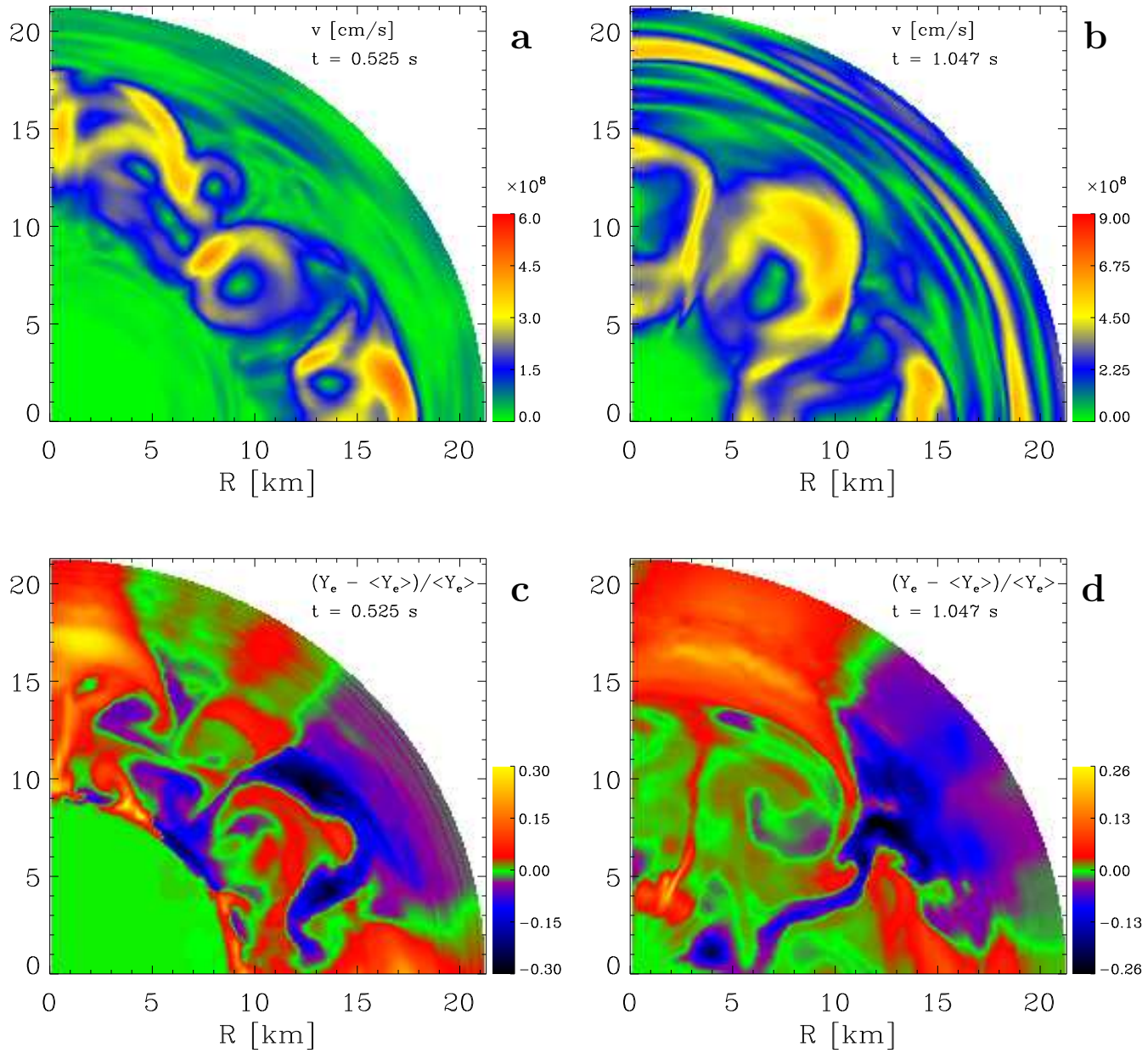


Fig. 3. Panels **a** and **b** show the absolute values of the velocity for the 2D simulation at times $t = 0.525$ s and $t = 1.047$ s, respectively, with the grey scale in units of 10^8 cm/s. Time is measured from the start of the simulation which is at about 25 ms after core bounce. The computation was performed in an angular wedge of 90° between $+45^\circ$ and -45° around the equatorial plane. The protoneutron star has contracted to a radius of about 21 km at the given times. Panels **c** and **d** display the relative deviations of the electron fraction Y_e from the angular means $\langle Y_e \rangle$ at each radius for the same two instants. The maximum deviations are of the order of 30%. Lepton-rich matter rises while deleptonized material sinks in. Comparison of both times shows that the inner edge of the convective layer moves inward from about 8.5 km at $t = 0.525$ s to less than 2 km at $t = 1.047$ s.

layers where convective mixing flattens the S and Y_l gradients.

The convective pattern is extremely non-stationary and has most activity on large scales with radial coherence lengths of several km up to ~ 10 km and convective “cells” of 20° – 30° angular diameter, at some times even 45° (Fig. 3). Significant over- and undershooting takes place (grey regions in Fig. 1) and the convective mass motions create pressure waves and perturbations in the convectively stable neutron star interior and in the surface layers. The maximum convective velocities are usually $\sim 4 \cdot 10^8$ cm/s, but peak values of $\sim 10^9$ cm/s can be reached. These velocities are typically 5–10% of the average sound speed in the star. The kinetic energy of the convection is several 10^{49} erg at $t \lesssim 1$ s and climbs to $\sim 2 \cdot 10^{50}$ erg when the protoneutron star is fully convective. Relative deviations of Y_l from the angular mean can be several 10% (even 100%) in rising or sinking buoyant elements, and for S can reach 5% or more. Rising flows always have larger Y_l and S than their surroundings. Corresponding temperature and density fluctuations are only ~ 1 –3%. Due to these properties and the problems in applying the Ledoux criterion with angle-averaged S and Y_l straightforwardly, we suspect that it is hardly possible to describe the convective activity with a mixing-length treatment in a 1D simulation.

Our 2D simulation shows that convection in the protoneutron star can encompass the whole star within ~ 1 s and can continue for at least as long as the deleptonization takes place, possibly even longer. A deleptonization “wave” associated with the convectively enhanced transport moves towards the center of the protoneutron star. This reduces the timescale for the electron fraction Y_e to approach its minimum central value of about 0.1 from ~ 10 s in the 1D case, where the lepton loss proceeds much more gradually and coherently, to only ~ 1.2 s in 2D. With convection the entropy and temperature near the center rise correspondingly faster despite a similar contraction of the star in 1D and 2D (Fig. 4). Convection increases the total lepton number flux and the ν luminosities by up to a factor of 2 (Fig. 5) and therefore the emitted lepton number N_l and energy E_ν rise much more rapidly (Fig. 4). The convective energy (enthalpy plus kinetic energy) flux dominates the diffusive ν energy flux in the convective mantle after $t \gtrsim 250$ ms and becomes more than twice as large later. Since convection takes place somewhat below the surface, ν ’s take over the energy transport exterior to $\sim 0.9 M_\odot$. Thus the surface ν flux shows relative anisotropies of only 3–4%, in peaks up to $\sim 10\%$, on angular scales of 10° – 40° . Averaged over all directions, the neutrinospheric temperatures and mean energies $\langle \epsilon_{\nu_i} \rangle$ of the emitted ν_e and $\bar{\nu}_e$ are higher by 10–20% (Fig. 5).

3.1.3 Consequences

Convectively increased neutrino emission from the protoneutron star does not only have influence on the supernova explosion mechanism. It is also of crucial importance to understand the nucleosynthesis in the neutrino-heated supernova ejecta and in the neutrino-driven wind whose degree of neutronization is determined by the interaction with the ν_e and $\bar{\nu}_e$ fluxes. Absorptions of ν_e onto free neutrons increase the free proton abundance while captures of $\bar{\nu}_e$ onto protons make the matter more *n*-rich.

As discussed above, convective neutrino transport in the nascent neutron star accelerates the deleptonization of the protoneutron star drastically. This means that during the first second or so the ν_e number flux \mathcal{N}_{ν_e} is increased relative to the $\bar{\nu}_e$ number flux $\mathcal{N}_{\bar{\nu}_e}$. If the protoneutron star atmosphere (where the neutrinospheres

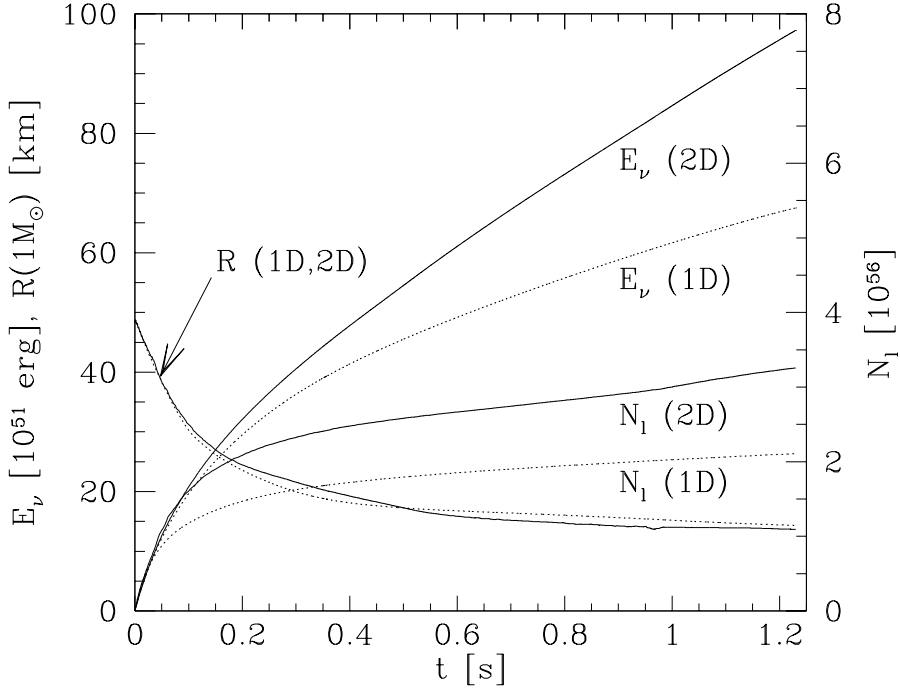


Fig. 4. Radius of the $M = 1 M_{\odot}$ mass shell and total lepton number N_1 and energy E_{ν} radiated away by neutrinos vs. time for the 2D (solid) and 1D (dotted) simulations.

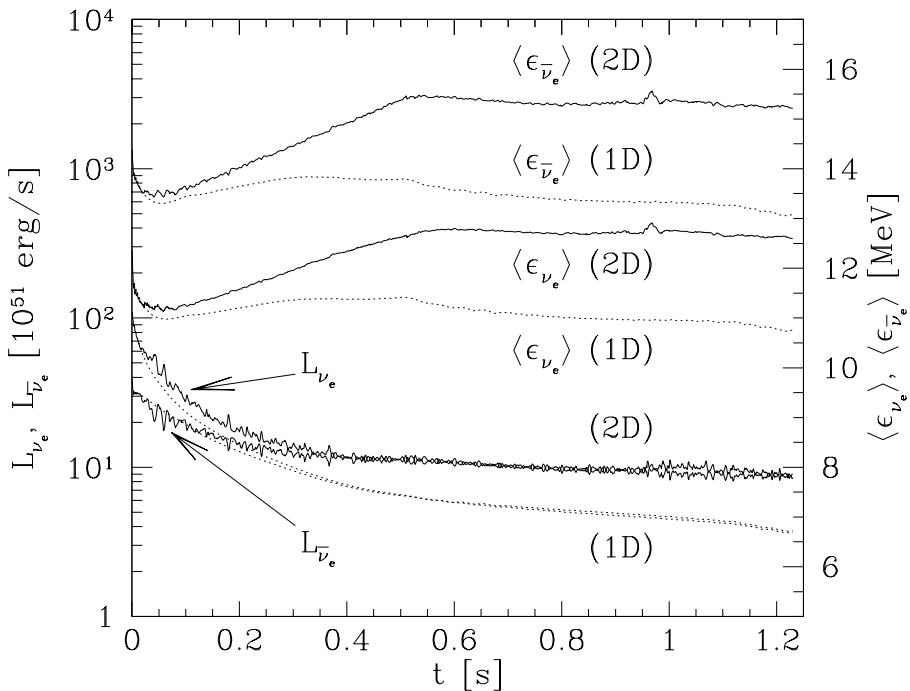


Fig. 5. ν_e and $\bar{\nu}_e$ luminosities and mean energies vs. time for the 2D simulation (solid) compared with the 1D run (dotted).

are located) is not convective but a radiative layer sitting on top of a convective region, then it can be shown (Keil et al. 1996) that the ratio of the average energies of $\bar{\nu}_e$ and ν_e , $\langle \epsilon_{\bar{\nu}_e}^n \rangle / \langle \epsilon_{\nu_e}^n \rangle$ (n is an arbitrary power), is not influenced very much by the convective activity deeper inside the star. In that case it is easy to see that the electron fraction in the ejecta, $Y_e^{\text{ej}} \approx 1 / [1 + (\mathcal{N}_{\bar{\nu}_e} \langle \epsilon_{\bar{\nu}_e}^2 \rangle) / (\mathcal{N}_{\nu_e} \langle \epsilon_{\nu_e}^2 \rangle)]$ (Qian & Woosley 1996), will increase when the ratio $\mathcal{N}_{\bar{\nu}_e} / \mathcal{N}_{\nu_e}$ decreases. Keil et al. (1996) found that this is indeed the case before about 0.4 s after shock formation. This effect offers a solution of the overproduction problem of $N = 50$ nuclei in current supernova models (see Hoffman et al. 1996, McLaughlin et al. 1996).

Because the opacity of the protoneutron star increases for ν_e (which are absorbed on neutrons) but decreases for $\bar{\nu}_e$ (absorbed on protons) with progressing neutronization of the matter, the accelerated neutronization of the convective protoneutron star will lead to a more rapid increase of $\langle \epsilon_{\bar{\nu}_e} \rangle$ relative to $\langle \epsilon_{\nu_e} \rangle$ than in 1D models at times later than about 1 s. This will favor a faster drop of Y_e^{ej} and thus might help to produce the n -rich conditions required for a possible r-processing in the high-entropy neutrino-driven wind (for details, see Woosley et al. 1994, Takahashi et al. 1994).

Without any doubt, an increase of the neutrino luminosities by a factor of ~ 2 during the first second after core bounce may be decisive for a successful explosion via the neutrino-heating mechanism. This will have to be investigated in future multi-dimensional simulations where not only the evolution of the protoneutron star is followed but the whole collapsed star is included. Parametric 1D and 2D studies with varied neutrino luminosities carried out by Janka & Müller (1995a, 1996) have already demonstrated the sensitivity of the explosion to changes of the luminosity of the order of some 10%. In the next section these results will be addressed.

3.2 Two-dimensional simulations of convection in the neutrino-heated region

Herant et al. (1992) first demonstrated by a hydrodynamical simulation that strong, turbulent overturn occurs in the neutrino-heated layer outside of the protoneutron star and that this helps the stalled shock front to start re-expansion as a result of energy deposition by neutrinos. Although the existence and fast growth of these instabilities was confirmed by Janka & Müller (1994, 1995a, 1996) the results of their simulations in 1D and in 2D indicated a very strong sensitivity to the conditions at the protoneutron star and to the details of the description of neutrino interactions and neutrino transport. Since the knowledge about the high-density equation of state in the nascent neutron star and about the neutrino opacities of dense matter is incomplete (see Sect. 2.1), the influence of a contraction of the neutron star and of the size of the neutrino fluxes on the evolution of the explosion has been tested by systematic studies.

In the following we shortly report the main conclusions that can be drawn from our set of 1D and 2D models with different core-neutrino luminosities and with varied temporal contraction of the inner boundary (Janka & Müller 1996).

3.2.1 Numerical implementation

The inner boundary was placed somewhat inside the neutrinosphere and was used instead of simulating the evolution of the very dense inner core of the nascent neutron star. This gave us the freedom to set the neutrino fluxes to chosen values at the

inner boundary and also enabled us to follow the 2D simulations until about one second after core bounce with a reasonable number ($\mathcal{O}(10^5)$) of time steps and an “acceptable” computation time, i.e. several 100 h on one processor of a Cray-YMP with a grid of 400×90 zones and a highly efficient implementation of the microphysics. Note that doubling the angular resolution multiplies the computational load by a factor of about 4!

Our simulations started at ~ 25 ms after shock formation from an initial model evolved through core collapse and bounce by Bruenn (1993). Boundary motion, luminosities of all neutrino kinds, and non-thermal neutrino spectra were time-dependent and mimiced the behavior in Bruenn (1993) and in Newtonian computations by Bruenn et al. (1995). Except for Doppler-shift and gravitational redshift the neutrino fluxes were kept constant with radius and did not include accretion luminosity. Neutrinos interact with matter by scattering on e^\pm , n , p , α , and nuclei, by neutrino pair processes, and ν_e and $\bar{\nu}_e$ also by the β -reactions. The reaction rates were evaluated by using Monte Carlo calibrated variable Eddington factors that depended on the density gradient at the neutron star surface. Inside the neutrinosphere reactive equilibrium between neutrinos and matter can be established. Our EOS described e^\pm as arbitrarily relativistic, ideal Fermi gases and n , p , α , and a representative nucleus as ideal Boltzmann gases in NSE (good at $\rho \lesssim 5 \times 10^{13}$ g/cm³ for temperatures $T \gtrsim 0.5$ MeV). 2D computations were performed with the Eulerian *Prometheus* code (up to 1° resolution and 400×180 zones), 1D runs with a Lagrangian method (details in Janka & Müller 1996).

3.2.2 Results for spherically symmetric models

The evolution of the stalled, prompt shock in 1D models turned out to be extremely sensitive to the size of the neutrino luminosities and to the corresponding strength of neutrino heating exterior to the gain radius. In models with successively higher core neutrino fluxes the shock is driven further and further out to larger maximum radii during a phase of ~ 100 –150 ms of slow expansion. Nevertheless, it finally recedes again to become a standing accretion shock at a much smaller radius (Fig. 6, dotted lines; see also Fig. 8). For a sufficiently high threshold luminosity, however, neutrino heating is strong enough to cause a successful explosion (Fig. 6, solid lines). For even higher neutrino fluxes the explosion develops faster and gets more energetic. In case of our $15 M_\odot$ star with $1.3 M_\odot$ Fe-core (Woosley et al. 1988) we find that explosions occur for ν_e and $\bar{\nu}_e$ luminosities above 2.2×10^{52} erg/s in case of a contracting inner boundary (to mimic the shrinking protoneutron star), but of only 1.9×10^{52} erg/s when the radius of the inner boundary is fixed.

The transition from failure to explosion requires the neutrino luminosities to exceed some threshold value. Yet, this is not sufficient. High neutrino energy deposition has to be maintained for a longer period of time to ensure high pressure behind the shock. If the decay of the neutrino fluxes is too fast, e.g., if a significant fraction of the neutrino luminosity comes from neutrino emission by spherically accreted matter, being shut off when the shock starts to expand, then the outward shock propagation may break down again and the model fizzles. Continuous shock expansion needs a sufficiently strong push from the neutrino-heated matter until the material behind the shock has achieved escape velocity and does not need pressure support to make its way out.

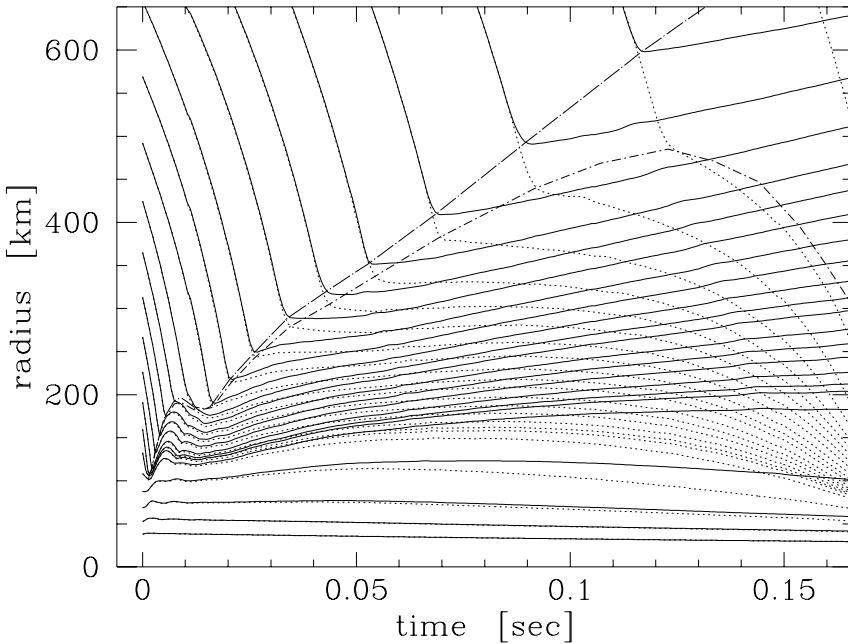


Fig. 6. Radial positions of mass shells of a marginally exploding model (solid lines) with initial neutrino luminosities from the lower boundary of $2.2 \cdot 10^{52}$ erg/s and of a still unsuccessful 1D model (dotted lines; initial boundary luminosities $2.1 \cdot 10^{52}$ erg/s) versus time after core bounce. The thick broken lines mark the shock positions.

This contradicts a recent suggestion by Burrows & Goshy (1993) that the explosion can be viewed as a global instability of the star that, once excited, inevitably leads to an explosion. The analysis by Burrows & Goshy may allow one to estimate the radius of shock stagnation when stationarity applies. The start-up phase of the explosion, however, can hardly be described by steady-state assumptions, because the timescales of shock expansion, of neutrino cooling and heating, and of temperature and density changes between neutron star and shock are all of the same order, although long compared to the sound crossing time and (possibly) shorter than the characteristic times of luminosity changes and variations of the mass accretion rate into the shock. In particular, due to the high sound speed and rather slow shock expansion the shock propagation is very sensitive to changes of the conditions in the neutrino-heated layer. A contraction of the neutron star or enhanced cooling of the gas inside the gain radius accelerate the advection of matter through the gain radius and reduce the time the postshock material is heated. This is harmful to the outward motion of the shock just as a moderate decline of the neutrino fluxes can be.

3.2.3 Results for two-dimensional models

In spherical symmetry the expansion of the neutrino-heated matter and of the shock can occur only when also the overlying material is lifted in the gravitational field of the neutron star. In the multi-dimensional case this is different. Blobs and lumps of heated matter can rise by pushing colder material aside and cold material from the region behind the shock can get closer to the zone of strongest neutrino heating to readily absorb energy. Also, when buoyancy forces drive hot matter outward, the

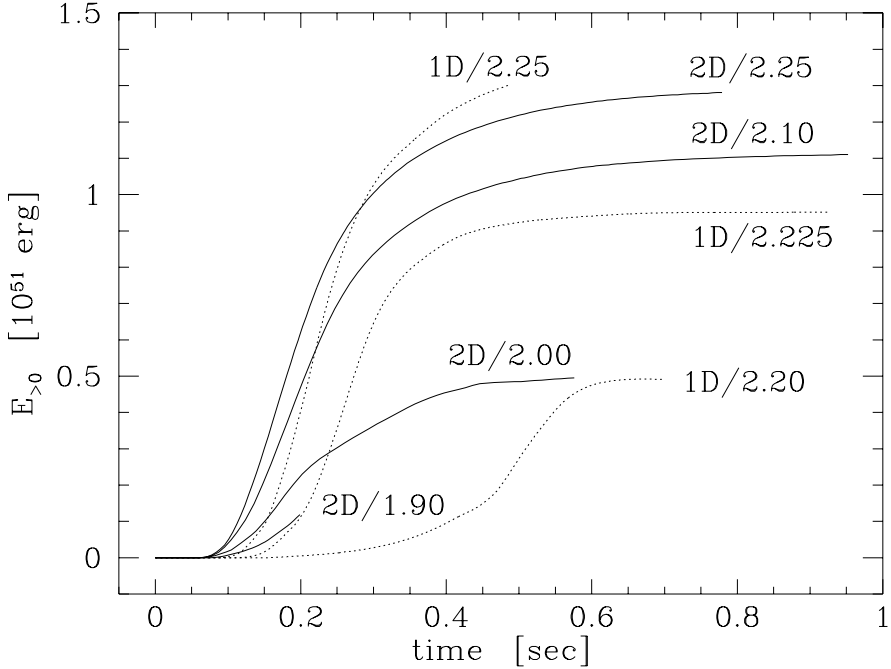


Fig. 7. Explosion energies vs. time after the start of the simulations (~ 25 ms after bounce) for exploding 1D (dotted) and 2D models (solid). The numbers denote the initial ν_e and $\bar{\nu}_e$ (approximately) luminosities in 10^{52} erg/s.

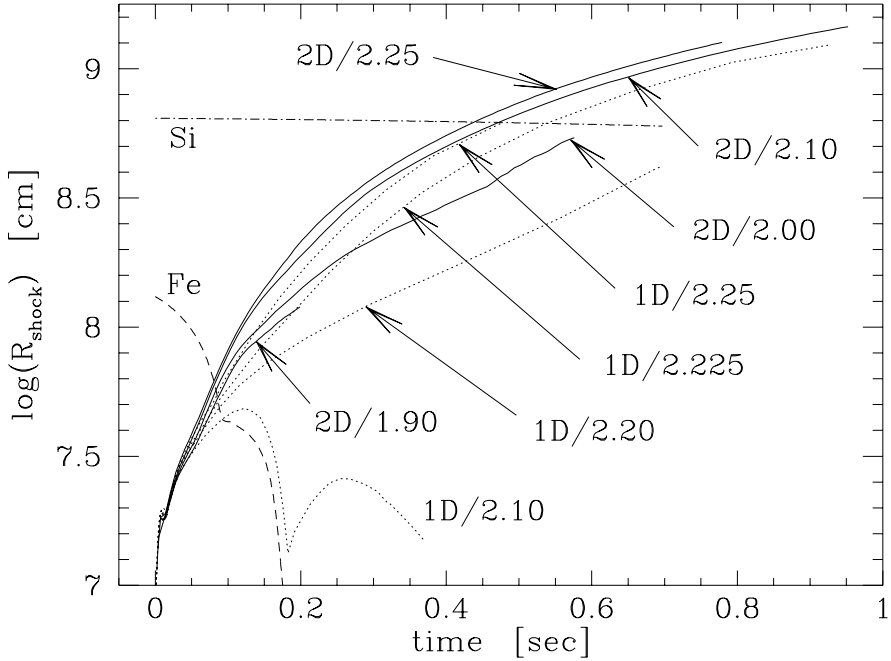


Fig. 8. Shock positions vs. time after core bounce for the exploding one-dimensional (“1D”, dotted lines) and two-dimensional (“2D”, solid lines) models of Fig. 7. The numbers indicate the size of the initial ν_e (and $\bar{\nu}_e$, approximately) luminosities in units of 10^{52} erg/s. In addition, the result for the unsuccessful 1D model with initial boundary luminosities of $2.1 \cdot 10^{52}$ erg/s is depicted. The dashed and dash-dotted curves mark the mass shells that correspond to the outer boundaries of Fe-core and Si-shell, respectively, for the latter model.

energy loss by re-emission of neutrinos is significantly reduced. Thus overturn of low-entropy and high-entropy gas increases the efficiency of neutrino energy deposition outside the radius of net energy gain and leads to explosions in 2D already for lower neutrino fluxes than in the spherically symmetrical case. Our models, however, do not show the existence of a “convective cycle” or “convective engine” (Herant et al. 1994) that transports energy from the heating region into the shock. The matter between protoneutron star and shock is subject to strong neutrino heating and cooling and our high-resolution calculations reveal a turbulent, unordered, and dynamically changing pattern of rising and sinking lumps of material with very different thermodynamical conditions and no clear indication of inflows of cool gas and outflows of hot gas at well-defined thermodynamical states.

2D models explode for core neutrino luminosities which cannot produce explosions in 1D. There is a window of neutrino fluxes with a width of $\sim 20\%$ of the threshold luminosity for explosions in 1D, where convective overturn between gain radius and shock is a significant help for shock revival. For lower neutrino fluxes even convective overturn cannot ensure strong explosions but the explosion energy gets very low. We do not find a continuous “accumulation” (Herant et al. 1994) of energy in the convective shell until an explosion energy typical of a type-II supernova is reached. For neutrino fluxes that cause powerful explosions already in 1D, turbulent overturn occurs but is not crucial for the explosion. In fact, in this case the fast rise of bubbles of heated material leads to a less vigorous start of the explosion and to the saturation of the explosion energy at a somewhat lower level (Fig. 7). The explosion energy, defined as the *net energy of the expanding matter at infinity*, does not exceed 10^{50} erg earlier than after ~ 100 ms of neutrino heating. This is the characteristic timescale of neutrinos to transfer an amount of energy to the material that is roughly equal to its gravitational binding energy and it is also the timescale that the convective overturn between gain radius and shock needs to develop to its full strength. It is not possible to determine or predict the final explosion energy of the star from a short period of only 100–200 ms after shock formation. Typically, the increase of the explosion energy with time levels off not before 400–500 ms after bounce, followed by only a very slow increase due to the much smaller contributions of the few $10^{-3} M_{\odot}$ of matter blown away from the protoneutron star in the neutrino wind (Fig. 7). Since the wind material is heated slowly and can expand as soon as the internal energy per nucleon roughly equals its gravitational binding energy, the matter does not have a large kinetic energy at infinity.

Although the global evolution of powerful explosions in 2D, i.e., the increase of the explosion energy with time (Fig. 7), the shock radius as a function of time (Fig. 8), or even the amount of ^{56}Ni produced by explosive nucleosynthesis, is not much different from energetic explosions of spherically symmetrical models, the structure of the shock and of the thick layer of expanding, dense matter behind the shock clearly bear the effects of the turbulent activity. The shock is deformed on large scales and its expansion velocity into different directions varies by $\sim 20\text{--}30\%$. The material behind the shock reveals large-scale inhomogeneities in density, temperature, entropy, and velocity, these quantities showing contrasts of up to a factor of 3. The typical angular scale of the largest structures is $\sim 30^\circ\text{--}45^\circ$. We do not find that the turbulent pattern tries to gain power on the largest possible scales and to evolve into the lowest possible mode, $l = 1$ (Herant et al. 1992, 1994). Turbulent motions are still going

on in the extended, dense layer behind the shock when we stop our calculations at ~ 1 s after bounce. We consider them as possible origin of the anisotropies, inhomogeneities, and non-uniform distribution of radioactive elements which were observed in SN 1987A. The contrasts behind the shock are about an order of magnitude larger than the artificial perturbations that were used in hydrodynamical simulations to trigger the growth of Rayleigh-Taylor instabilities in the stellar mantle and envelope.

3.2.4 From core bounce to one second

Convective overturn in the neutrino-heated layer around the protoneutron star develops within ~ 50 – 100 ms after shock formation. About 200– 300 ms after bounce neutrinos have deposited a sizable amount of energy in the material below the shock front. The turbulent layer begins to move away from the region of strongest neutrino heating and to expand outward behind the accelerating shock (Fig. 9). At this time turbulent activity around and close to the protoneutron star comes to an end. An extended phase of convection and accretion outside the protoneutron star does not occur. Inflows of low-entropy, p -rich gas from the postshock region towards the neutrino-heated zone are not accreted onto the neutron star. Although the gas loses lepton number while falling in, it does not get as n -rich as the material inside the gain radius. In addition, neutrino heating and mixing with the surrounding, high-entropy gas increase the entropy in the downflows. Both high electron (proton) concentration and high entropy have a stabilizing effect and prevent the penetration of the gas through the gain radius into the cooler and more n -rich surface layer of the protoneutron star.

At ~ 400 – 500 ms the protoneutron star has become quite compact and the density outside has dropped appreciably. This indicates the formation of the high-entropy, low-density “hot-bubble” region (Bethe & Wilson 1985) and the phase of small mass loss from the nascent neutron star in the neutrino-driven wind, accompanied by slowly increasing entropies. The wind accelerates because of the steepening density decline away from the shrinking neutron star. The faster expansion and push of the wind create a density inversion between the massive, slow, inert shell behind the shock and the evacuating hot-bubble region. Around the time the outgoing supernova shock passes the entropy and composition step of the Si-O interface at ~ 5700 km (see Fig. 8), this density inversion steepens into a strong reverse shock that forms a sharp discontinuity in the neutrino wind, slowing down the wind expansion from $> 2 \times 10^9$ cm/s to a few times 10^8 cm/s. Since the velocities of the wind and of the layer behind the shock decrease with time, it is possible that this reverse shock will trigger fallback of a significant fraction of the matter that was blown out in the neutrino wind. Once the infall of the outer wind material is initiated and the pressure support for the gas further out vanishes, inward acceleration might even enforce the fallback of more slowly moving parts of the dense shell behind the supernova shock.

Fallback of a significant amount of matter, ~ 0.1 to $0.2 M_\odot$, might be needed to solve two major problems in the current supernova models. On the one hand, due to the fast development of the explosion and the lack of an extended accretion phase, the protoneutron star formed at the center of the explosion has quite a small (initial) baryonic mass, only $\sim 1.2 M_\odot$ in case of our $15 M_\odot$ star with $1.3 M_\odot$ Fe-core. On the other hand, the yields of Fe-peak elements by explosive nucleosynthesis are incompatible with observational constraints for type-II supernovae as deduced

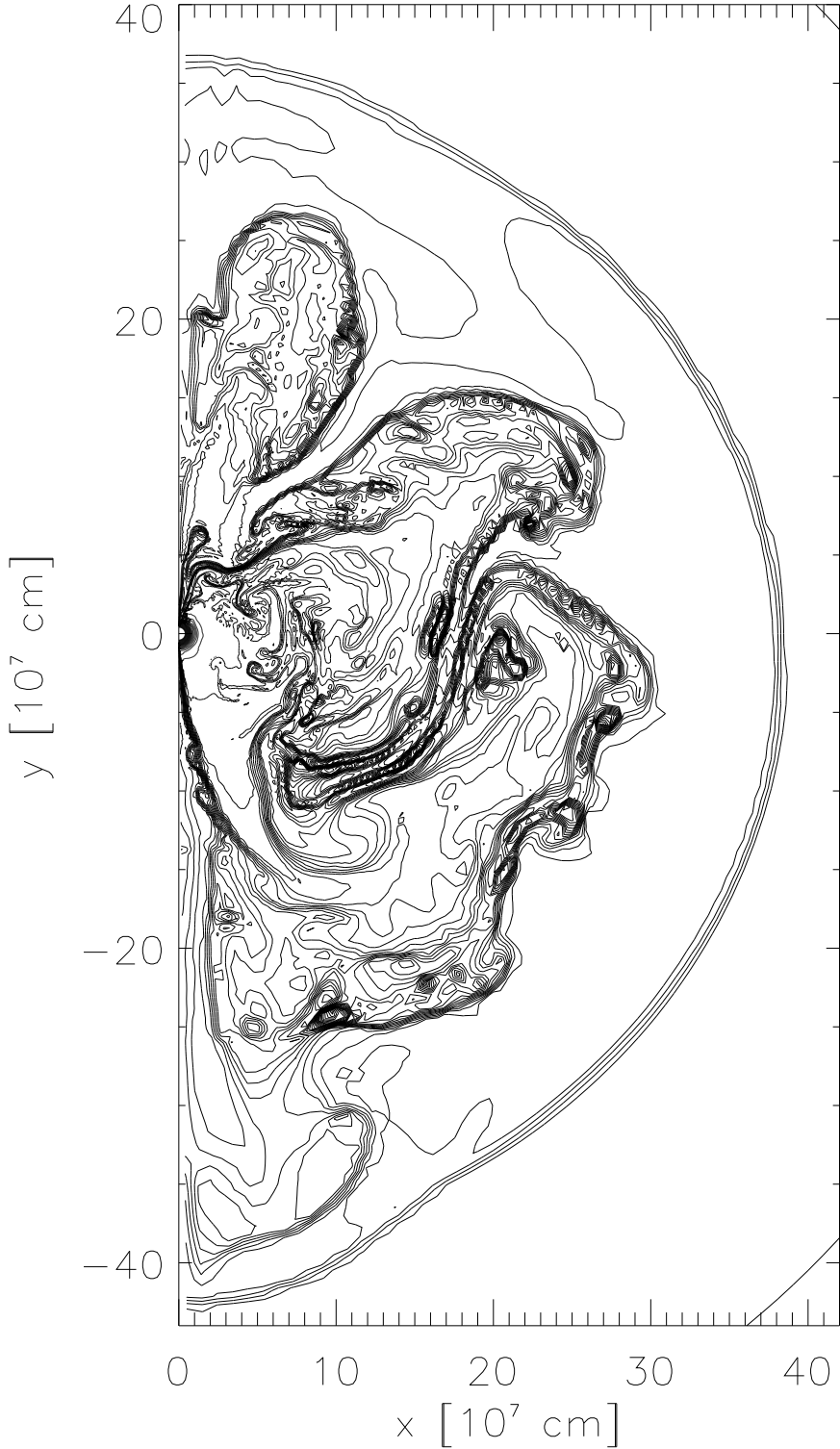


Fig. 9. A weakly exploding 2D model with an explosion energy of about $0.5 \cdot 10^{51}$ erg at a time $t = 377$ ms after bounce. The figure shows entropy contours, equidistantly spaced in steps of $0.5 k_B/\text{nucleon}$ between $5 k_B/\text{nucleon}$ and $16 k_B/\text{nucleon}$ and in steps of $1.0 k_B/\text{nucleon}$ between $16 k_B/\text{nucleon}$ and $23 k_B/\text{nucleon}$. The shock is located at about 3800 km. Clumpy structures, inhomogeneities, and vortex patterns caused by Kelvin-Helmholtz instabilities are visible along the boundaries between downflows of cold gas from the postshock region and hot, rising gas from the neutrino-heated zone around the protoneutron star at the coordinate center.

from terrestrial abundances and galactic evolution arguments. In case of powerful explosions with energies of $1\text{--}1.3 \times 10^{51}$ erg material of $\sim 0.2 M_\odot$ is heated to temperatures $T > 4.5 \times 10^9$ K and is ejected behind the shock during the early phase of the explosion. Only roughly half of this matter, $0.085\text{--}0.1 M_\odot$, has an electron fraction $Y_e > 0.49$ and will end up with ^{56}Ni as the dominant nucleosynthesis product. In that respect the models seem to match the observations quite well. Yet, only some part ($\sim 0.05 M_\odot$) of the matter that is shock-heated to $T > 4.5 \times 10^9$ K has $Y_e \gtrsim 0.495$ and will end up with relative abundance yields in acceptable agreement with solar-system values. The amount of ^{56}Ni produced in neutrino-driven explosions turns out to be correlated with the explosion energy. In case of more energetic explosions the shock is able to heat a larger mass to sufficiently high temperatures.

3.2.5 Consequences

Turbulent overturn between the zone of strongest neutrino heating and the supernova shock aids the re-expansion of the stalled shock and is able to cause powerful type-II supernova explosions in a certain, although rather narrow, window of core neutrino fluxes where 1D models do not explode. The turbulent activity outside and close to the protoneutron star is transient and between 300 and 500 ms after core bounce the (essentially) spherically symmetrical neutrino-wind phase starts and the turbulent shell moves outward behind the expanding supernova shock. Our 2D simulations do not show a long-lasting period of convection and accretion after core bounce. Only very little of the cool, low-entropy matter that flows down from the shock front to the zone of neutrino energy deposition is advected into the protoneutron star surface. Since the matter is p -rich and its entropy increases quickly due to neutrino heating, it stays in the heated region to gain more energy by neutrino interactions and to start rising again. The strong, large-scale inhomogeneities and anisotropies in the expanding layer behind the outward propagating shock front will probably help to explain the effects of macroscopic mixing seen in SN 1987A and can account for neutron star recoil velocities of a few 100 km/s (details in Janka & Müller 1994, 1995b).

Although the models develop energetic explosions for sufficiently high neutrino luminosities and produce an amount of ^{56}Ni that is in good agreement with observational constraints, the initial mass of the protoneutron star is clearly on the low side of the spectrum of measured neutron star masses. Moreover, the models eject $\sim 0.1\text{--}0.15 M_\odot$ of material with $Y_e < 0.495$, which implies an overproduction of certain elements in the Fe-peak by an appreciable factor compared with the nucleosynthetic composition in the solar system. The fallback of a significant fraction of this matter to the neutron star at a later stage would ease these problems. It is possible that the reverse shock which develops in our models will trigger this fallback on a timescale of seconds. Due to the strong inhomogeneities in the dense layer behind the shock this fallback could happen with considerable anisotropy and impart an additional kick to the neutron star (Janka & Müller 1995b).

On the other hand, it is hard to see how fallback could achieve a clean disentanglement of desirable and undesirable ejecta, in particular if one has in mind the turbulent activity and the mixing of different conditions present in the neutrino-heated layer. Nevertheless, it may still be that the observed nucleosynthetic composition of the interstellar medium reflects the accidental result of a delicate separation of

“good” and “bad” products of explosive nucleosynthesis during the early phases of the explosion. Alternatively, as discussed in Sect. 3.1.3, the contamination of the supernova ejecta with overproduced $N = 50$ nuclei could be more naturally and plausibly avoided if the luminosities of ν_e and $\bar{\nu}_e$ and therefore the degree of neutronization in the neutrino-heated material were modified by convection in the nascent neutron star.

4. Summary and discussion

Recent multi-dimensional simulations of type-II supernova explosions (Herant et al. 1994, Burrows et al. 1995, Janka & Müller 1996) have shown that convective overturn in the neutrino-heating region helps the explosion and can be crucial for the success of the delayed explosion mechanism. The net efficiency of neutrino energy deposition is increased when cold (low-entropy) material from behind the shock can move inward to the region of strongest heating, while at the same time heated (high-entropy) gas can rise outward and expand, thus reducing the energy loss by reemission of neutrinos. The delicate balance of neutrino heating and cooling which is present in the spherically symmetric case is avoided, and the neutrino luminosity that is required for sufficiently strong heating to obtain an explosion is lowered.

However, there is still a competition between the neutrino heating timescale and the timescale for the growth of the convective instability on the one hand and the advection timescale of matter from the shock through the gain radius (interior of which neutrino heating is superseded by neutrino cooling) towards the protoneutron star on the other. For too low neutrino luminosities the heating in the postshock region is not strong enough to ensure short growth timescales of the convective overturn. In this case the matter is advected downward through the gain radius faster than it is driven outward by buoyancy forces. Inside the gain radius the absorbed neutrino energy is quickly radiated away again by neutrino emission. Therefore convective overturn in the neutrino-heated region is crucial for the explosion only in a rather narrow window of luminosities. For higher core neutrino fluxes also spherically symmetrical models yield energetic explosions, while for lower luminosities even with convection no strong explosions occur. In any case, the success of the delayed explosion mechanism requires sufficiently large neutrino luminosities from the nascent neutron star for a sufficiently long time.

Moreover, all current supernova models have severe problems concerning the nucleosynthetic composition of the neutrino-heated ejecta. These show huge overproduction factors (up to the order of 100) for elements around neutron number $N = 50$, indicating that the ejecta are too neutron-rich. Several suggestions have been made to solve this problem, e.g., fallback of some of the early ejecta towards the neutron star during a later phase of the explosion (Herant et al. 1994), a longer delay of the explosion than obtained in current models which would reduce the amount of neutron-rich material due to the density decrease in the region between supernova shock and protoneutron star (Burrows & Hayes 1995), or a slightly underestimated electron fraction Y_e in the ejecta because of still unsatisfactorily treated neutrino transport which affects the computed ν_e and $\bar{\nu}_e$ spectra and thus the neutrino-matter interactions in the hot bubble region (Hoffman et al. 1996). While the latter might certainly be true and has to be investigated carefully (see Sect. 2.1), all of these suggestions

rely on some fine-tuning and effects which might be very unstable and sensitive to minor changes.

Strong convection inside the newly formed neutron star during the first few hundred milliseconds after core bounce and shock formation offers a remedy of both problems (Keil et al. 1996). Faster cooling of the protoneutron star by convective energy transport increases the total neutrino luminosities and therefore helps the neutrino energy deposition in the postshock layers. The accompanying enhanced deleptonization raises the ν_e number flux relative to the $\bar{\nu}_e$ number flux. This leads to more frequent absorptions of ν_e onto neutrons in the neutrino-heated gas and thus can establish a higher electron fraction in the material that carries the supernova energy during the early moments of the explosion. The final confirmation of this picture has still to be waited for until multi-dimensional supernova simulations have been performed that follow the protoneutron star *and* the surrounding progenitor star for a sufficiently long time.

Acknowledgements. The author would like to thank the organizers, in particular M. Locher, for the great hospitality and the opportunity to attend the summer school in Zuoz. This work was supported by the Sonderforschungsbereich 375-95 for Astro-Particle Physics of the Deutsche Forschungsgemeinschaft. The computations were performed on the CRAY-YMP 4/64 of the Rechenzentrum Garching.

References

Alexeyev E.N., et al., 1988, Phys. Lett. B205, 209
 Arnett W.D., 1988, ApJ 331, 337
 Arnett W.D., Bahcall J.N., Kirshner R.P., Woosley S.E., 1989, ARA&A 27, 629
 Arnett W.D., Fryxell B.A., Müller E., 1989, ApJ 341, L63
 Aschenbach B., Egger R., Trümper J., 1995, Nat 373, 587
 Barthelmy S., 1989, et al., IAU Circ. 4764
 Bethe H.A., Wilson J.R., 1985, ApJ 295, 14
 Bethe H.A., Brown G.E., Cooperstein J., 1987, ApJ 322, 201
 Bionta R.M., et al., 1987, Phys. Rev. Lett. 58, 1494 (IMB collaboration)
 Bruenn S.W., 1985, ApJS 58, 771
 Bruenn S.W., 1993, in: Nuclear Physics in the Universe, eds. M.W. Guidry and M.R. Strayer, IOP, Bristol, p. 31
 Bruenn S.W., Dineva T., 1996, ApJ 458, L71
 Bruenn S.W., Mezzacappa A., 1994, ApJ 433, L45
 Bruenn S.W., Mezzacappa A., Dineva T., 1995, Phys. Rep. 256, 69
 Burrows A., 1987, ApJ 318, L57
 Burrows A., Fryxell B.A., 1992, Sci 258, 430
 Burrows A., Fryxell B.A., 1993, ApJ 418, L33
 Burrows A., Goshy J., 1993, ApJ 416, L75
 Burrows A., Hayes J., 1995, Ann. N.Y. Acad. Sci. 759, 375
 Burrows A., Hayes J., Fryxell B.A., 1995, ApJ 450, 830
 Burrows A., Lattimer J.M., 1986, ApJ 307, 178
 Burrows A., Lattimer J.M., 1988, Phys. Rep. 163, 51
 Caraveo P.A., 1993, ApJ 415, L111

Colella P., Woodward P.R., 1984, *J. Comp. Phys.* 54, 174

Colgan S.W.J., Haas M.R., Erickson E.F., Lord S.D., Hollenbach D.J., 1994, *ApJ* 427, 874

Colgate S.A., Herant M., Benz W., 1993, *Phys. Rep.* 227, 157

Colgate S.A., White R.H., 1966, *ApJ* 143, 626

Cook W.R., et al., 1988, *ApJ* 334, L87

Den M., Yoshida T., Yamada Y., 1990, *Prog. Theor. Phys.* 83, 723

Dotani T., et al., 1987, *Nat* 330, 230

Erickson E.F., et al., 1988, *ApJ* 330, L39

Epstein R.I., 1979, *MNRAS* 188, 305

Frail D.A., Kulkarni S.R., 1991, *Nat* 352, 785

Fryxell B.A., Müller E., Arnett W.D., 1989, MPA-Preprint 449, Max-Planck-Institut für Astrophysik, Garching

Fryxell B.A., Müller E., Arnett W.D., 1991, *ApJ* 367, 619

Gehrels N., Leventhal M., MacCallum C.J., 1988, in: Nuclear Spectroscopy of Astrophysical Sources, eds. N. Gehrels and G. Share, AIP, New York, p. 87

Gudry M.W., 1996, talk at the workshop of the ‘European Centre for Theoretical Studies in Nuclear Physics’ on Physics of Supernovae and Neutron Stars, Trento, Italy, June 3–14, 1996

Haas M.R., et al., 1990, *ApJ* 360, 257

Hachisu I., Matsuda T., Nomoto K., Shigeyama T., 1990, *ApJ* 358, L57

Hachisu I., Matsuda T., Nomoto K., Shigeyama T., 1991, *ApJ* 368, L27

Harrison P.A., Lyne A.G., Anderson B., 1993, *MNRAS* 261, 113

Herant M., Benz W., 1991, *ApJ* 345, L412

Herant M., Benz W., 1992, *ApJ* 387, 294

Herant M., Benz W., Colgate S.A., 1992, *ApJ* 395, 642

Herant M., Benz W., Hix W.R., Fryer C.L., Colgate S.A., 1994, *ApJ* 435, 339

Hillebrandt W., 1987, in: High Energy Phenomena Around Collapsed Stars, NATO ASI C195, ed. F. Pacini, Reidel, Dordrecht, p. 73

Hirata K., et al., 1987, *Phys. Rev. Lett.* 58, 1490 (Kamiokande II collaboration)

Hoffman R.D., Woosley S.E., Fuller G.M., Meyer B.S., 1996, *ApJ* 460, 478

Janka H.-Th., 1993, in: Frontier Objects in Astrophysics and Particle Physics, eds. F. Giovanelli and G. Mannocchi, Società Italiana di Fisica, Bologna, p. 345

Janka H.-Th., 1995, in: Proc. of the Workshop on Astro-Particle Physics of the Sonderforschungsbereich 375, Ringberg Castle, Tegernsee, March 6–10, 1995, eds. A. Weiss, G. Raffelt, W. Hillebrandt, F. von Feilitzsch, Technische Universität München, p. 154

Janka H.-Th., Müller E., 1993, in: Frontiers of Neutrino Astrophysics, eds. Y. Suzuki and K. Nakamura, Universal Academy Press, Tokyo, p. 203

Janka H.-Th., Müller E., 1994, *A&A* 290, 496

Janka H.-Th., Müller E., 1995a, *ApJ* 448, L109

Janka H.-Th., Müller E., 1995b, *Ann. N.Y. Acad. Sci.* 759, 269

Janka H.-Th., Müller E., 1996, *A&A* 306, 167

Janka H.-Th., Keil W., Raffelt G., Seckel D., 1996, *Phys. Rev. Lett.* 76, 2621

Keil W., 1996, Ph.D. Thesis, TU München (in preparation)

Keil W., Janka H.-Th., 1995, *A&A* 296, 145

Keil W., Janka H.-Th., Müller E., 1996, MPA-preprint 971, *ApJL*, in press

Keil W., Janka H.-Th., Raffelt G., 1995, *Phys. Rev. D* 51, 6635

Lattimer J.M., Swesty F.D., 1991, *Nucl. Phys.* A535, 331

Li H., McCray R., Sunyayev R.A., 1993, *ApJ* 419, 824

Lyne A.G., Lorimer D.R., 1994, *Nat* 369, 127

Mahoney W.A., et al., 1988, *ApJ* 334, L81

Matz S.M., et al., 1988, *Nat* 331, 416

Mayle R.W., Wilson J.R., 1988, *ApJ* 334, 909

McLaughlin G.C., Fuller G.M., Wilson J.R., 1996, *ApJ*, in press

Miller D.S., Wilson J.R., Mayle R.W., 1993, *ApJ* 415, 278

Müller E., 1993, in: Proc. of the 7th Workshop on Nuclear Astrophysics (Ringberg Castle, March 22-27, 1993), eds. W. Hillebrandt and E. Müller, Report MPA/P7, Max-Planck-Institut für Astrophysik, Garching, p. 27

Müller E., Fryxell B.A., Arnett W.D., 1991, in: ESO/EIPC Workshop on SN 1987A and other Supernovae, ESO Workshop and Conference Proceedings No. 37, eds. I.J. Danziger and K. Kjär, ESO, Garching, p. 99

Müller E., Janka H.-Th., 1994, in: Reviews in Modern Astronomy 7, Proceedings of the International Scientific Conference of the AG (Bochum, Germany, 1993), ed. G. Klare, Astronomische Gesellschaft, Hamburg, p. 103

Qian Y.-Z., Woosley S.E., 1996, *ApJ*, in press

Raffelt G., Seckel D., 1991, *Phys. Rev. Lett.* 67, 2605

Rank D.M., 1988, et al., *Nat* 331, 505

Sandie W.G., et al., 1988, *ApJ* 334, L91

Shigeyama T., Nomoto K., 1990, *ApJ* 360, 242

Shigeyama T., Nomoto K., Hashimoto M., 1988, *A&A* 196, 141

Shimizu T., Yamada S., Sato K., 1993, *PASJ* 45, L53

Shimizu T., Yamada S., Sato K., 1994, *ApJ* 432, L119

Sigl G., 1996, *Phys. Rev. Lett.* 76, 2625

Spyromilio J., Meikle W.P.S., Allen D.A., 1990, *MNRAS* 242, 669

Stewart R.T., Caswell J.L., Haynes R.F., Nelson G.J., 1993, *MNRAS* 261, 593

Sumiyoshi K., Suzuki H., Toki H., 1995, *A&A* 303, 475

Sunyaev R.A., et al., 1987, *Nat* 330, 227

Suzuki H., 1989, Ph.D. Thesis, Univ. of Tokyo

Takahashi K., Witt J., Janka H.-Th., 1994, *A&A* 286, 857

Taylor J.H., Manchester R.N., Lyne A.G., 1993, *ApJS* 88, 529

Teegarden B.J., et al., 1989, *Nat* 339, 122

Tueller J., et al., 1990, *ApJ* 351, L41

Wilson J.R., Mayle R.W., 1988, *Phys. Rep.* 163, 63

Wilson J.R., Mayle R.W., 1989, in: The Nuclear Equation of State, Part A, eds. W. Greiner and H. Stöcker, Plenum Press, New York, p. 731

Wilson J.R., R.W. Mayle, 1993, *Phys. Rep.* 227, 97

Wilson R.B., et al., 1988, in: Nuclear Spectroscopy of Astrophysical Sources, eds. N. Gehrels and G. Share, AIP, New York, p. 66

Witteborn F., et al., 1989, *ApJ* 338, L9

Witti J., Janka H.-Th., Takahashi K., 1994, *A&A* 286, 841

Woosley S.E., 1988, *ApJ* 330, 218

Woosley S.E., Hoffman R.D., 1992, *ApJ* 395, 202

Woosley S.E., Pinto P.A., Enzman L., 1988, *ApJ* 324, 466

Woosley S.E., Wilson J.R., Mathews G.J., Hoffman R.D., Meyer B.S., 1994, *ApJ* 433, 229

Yamada Y., Nakamura T., Oohara K., 1990, *Prog. Theor. Phys.* 84, 436

Yamada S., Shimizu T., Sato K., 1993, *Prog. Theor. Phys.* 89, 1175